doi.org/10.36721/PJPS.2026.39.7.202.1

miR-152-3p inhibits triple-negative breast cancer cell progression by targeting signal transducer and activator of transcription 3, nuclear factor kappa B subunit p65 and adenylate cyclase 6

Yan Cheng[1]* and Yingyao Quan[2]
[1]Department of Anesthesiology, Anji County Traditional Chinese Medicine Hospital, Huzhou, Zhejiang, 313399, China
[2]Department of Anesthesiology, Maternal and Child Health Hospital of Hubei Province, Wuhan, Hubei, 430070, China

Abstract: **Background**: Triple-negative breast cancer (TNBC) is the most aggressive breast cancer subtype and currently lacks defined therapeutic targets. Although miR-152-3p functions as a tumor suppressor in various cancers, its specific mechanism and regulatory network in TNBC remain poorly understood. **Objectives**: To investigate the expression and tumor-suppressive function of miR-152-3p in TNBC cells and to elucidate its mechanism of targeting STAT3, RELA and ADCY6. **Methods**: miR-152-3p expression was compared between MDA-MB-231 and MCF-10A cells using qRT-PCR. MDA-MB-231 cells were transfected with miR-152-3p mimics or inhibitors and cell proliferation, apoptosis and invasion were assessed by MTT assay, flow cytometry and Transwell assay, respectively. Direct target interactions were validated by a dual-luciferase reporter assay, and protein levels of STAT3, RELA, and ADCY6 were examined by Western blot. Key findings were further validated in Hs 578T cells. **Results**: miR-152-3p expression was significantly downregulated in TNBC cells. Overexpression of miR-152-3p markedly inhibited proliferation and invasion while promoting apoptosis in MDA-MB-231 cells. Dual-luciferase reporter assays confirmed that miR-152-3p directly binds to the 3‘untranslated regions of STAT3, RELA and ADCY6. Overexpression of miR-152-3p significantly reduced STAT3 and RELA protein levels while upregulating ADCY6 expression. Rescue experiments demonstrated that restoration of STAT3 expression partially reversed the tumor-suppressive effects of miR-152-3p. These findings were recapitulated in Hs 578T cells, suggesting generalizability across TNBC subtypes. **Conclusion**: miR-152-3p suppresses TNBC progression by downregulating STAT3/RELA and upregulating ADCY6, thereby activating cAMP signaling. These findings provide a foundation for further investigation into the potential of miR-152-3p as a multi-target therapeutic strategy for TNBC.

Keywords: ADCY6; Biological activity; miR-152-3p; RELA; STAT3; TNBC MDA-MB-231 cells

Submitted on 14-12-2025 – Revised on 05-03-2026 – Accepted on 10-03-2026

INTRODUCTION

Breast cancer is one of the most prevalent malignancies worldwide, with approximately 1.2 million new cases of breast cancer diagnosed annually, of which an estimated 170,000 are triple-negative breast cancer (TNBC) (Giaquinto *et al*., 2024; Sammons *et al*., 2025). TNBC is a particularly aggressive subtype characterized by early invasion, high metastatic potential, pronounced heterogeneity and the absence of well-defined therapeutic targets, contributing to the highest mortality rate among breast cancer subtypes. Therefore, elucidating the molecular mechanisms underlying TNBC pathogenesis and identifying novel therapeutic strategies are of critical importance (Deng *et al*., 2024).

MicroRNAs (miRNAs) are a class of small non-coding RNAs approximately 17–25 nucleotides in length that function as key post-transcriptional regulators of gene expression. By binding to the 3' untranslated region (3’UTR) of target mRNAs, miRNAs induce mRNA degradation or translational repression, thereby modulating diverse biological processes, including proliferation, apoptosis, invasion and metastasis (Yang *et al*., 2022). Among these, miR-152-3p has been reported to act as a tumor suppressor in multiple cancer types (Turijan-Espinoza *et al*., 2026). However, its specific function, downstream targets and regulatory network in TNBC remain largely unexplored.

Signal transducer and activator of transcription 3 (STAT3) and nuclear factor kappa B (NF-κB) are two critical pro-survival and pro-inflammatory signaling pathways. STAT3 is a cancer-associated transcription factor abundantly expressed in the cytoplasm, where it regulates cell proliferation and apoptosis (Hu *et al*., 2024; Arun *et al*., 2024). NF-κB, particularly its p65/RELA subunit, is closely associated with tumor invasion, metastasis and chemoresistance (Mufidah *et al*., 2025). Notably, STAT3 and NF-κB pathways interact at the transcriptional level to form a core signaling network that sustains the malignant phenotype. Cyclic adenosine monophosphate (cAMP) serves as a second messenger that regulates downstream effectors and modulates various physiological processes (Patritti *et al*., 2022; Gao *et al*., 2022). Activation of cAMP signaling has been shown to suppress proliferation and induce apoptosis in lymphoma cells (Ethiraj *et al*., 2022). Adenylate cyclase 6 (ADCY6), a cAMP-producing enzyme, directly influences intracellular cAMP levels and protein kinase A (PKA) activity and has been implicated in breast cancer progression (Guo *et al*., 2022).

**Corresponding author:* e-mail: tuoye7315351933@126.com

Based on these findings, it was hypothesized that miR-152-3p may exert potent tumor-suppressive effects by simultaneously targeting and coordinately regulating STAT3, NF-κB and cAMP-PKA signaling pathways. To test this hypothesis, the expression, function and molecular mechanism of miR-152-3p in TNBC were systematically investigated. This study moves beyond the traditional single-target paradigm and provides evidence that miR-152-3p may suppress TNBC through multi-target synergistic regulation, offering potential insights into miRNA-based combination therapeutic strategies.

MATERIALS AND METHODS

Cell Lines

Breast epithelial cells MCF-10A, TNBC cell lines MDA-MB-231 and Hs 578T, as well as the estrogen receptor-positive (ER+) breast cancer cell line MCF-7 (used as a non-TNBC control), were purchased from the American Type Culture Collection (ATCC) cell bank (United States).

In this study, MDA-MB-231 cells were selected as the primary TNBC model because this cell line is among the most commonly used and well-characterized systems worldwide for investigating TNBC biology and metastasis, and it exhibits distinct molecular features of basal-like TNBC. To validate the generalizability of key findings, Hs 578T cells were included as a secondary TNBC cell line for core validation. In addition, MCF-7 cells [luminal A subtype, ER+/progesterone receptor-positive (PR+)] were used as a non-TNBC control to assess the study's findings for subtype specificity.

Reagents and instruments

MiR-152-3p mimics and a negative control (miR-NC) were purchased from Shanghai Jikai Gene Chemical Technology Co., Ltd. (Shanghai, China). Antibodies against STAT3 (catalog #9139), RELA (catalog #8242), and ADCY6 (catalog #13195) were purchased from Cell Signaling Technology (CST, Danvers, MA, USA). β-Actin antibody (catalog #A1978) was from Sigma-Aldrich (St. Louis, MO, USA). HRP-conjugated secondary antibodies (anti-rabbit, catalog #7074; anti-mouse, catalog #7076) were also from CST. Lipofectamine 3000 transfection reagent (catalog #L3000015) and TRIzol reagent (catalog #15596026) were from Invitrogen (Carlsbad, CA, USA). Mir-X miRNA First-Strand Synthesis Kit (catalog #638315) was from Takara Bio (Kusatsu, Japan). SYBR Green Master Mix (catalog #4367659) was from Applied Biosystems (Foster City, CA, USA). MTT (catalog #M2128) and DMSO (catalog #D8418) were from Sigma-Aldrich. Annexin V-FITC/PI Apoptosis Detection Kit (catalog #556547) was from BD Biosciences (San Jose, CA, USA). Matrigel (catalog #356234) and Transwell chambers (8.0 μm pore size, catalog #3422) were from Corning (Corning, NY, USA). Dual-Luciferase® Reporter Assay System (catalog #E1910) and pRL-TK Renilla luciferase control plasmid (catalog #E2241) were from Promega (Madison, WI, USA). pGL3-Promoter vector (catalog #E1761) was also from Promega. RIPA lysis buffer (catalog #P0013B) and BCA protein assay kit (catalog #P0012) were from Beyotime Biotechnology (Shanghai, China). Protease and phosphatase inhibitor cocktail (catalog #04906837001) was from Roche (Basel, Switzerland). PVDF membranes (0.45 μm, catalog #IPVH00010) were from Millipore (Burlington, MA, USA). SuperSignal™ West Pico PLUS chemiluminescent substrate (catalog #34580) was from Thermo Scientific (Waltham, MA, USA).

Experimental method

Cell culture

Human breast epithelial cells (MCF-10A), triple-negative breast cancer (TNBC) cell lines (MDA-MB-231 and Hs 578T) and MCF-7 cells were all purchased from the ATCC cell bank (USA) and authenticated by short tandem repeat (STR) profiling. All cells were cultured in their recommended complete media: MCF-10A cells were maintained in MEGM™ BulletKit™ (Lonza, CC-3150); MDA-MB-231 and Hs 578T cells were cultured in Leibovitz‘s L-15 medium (Gibco, 11415064) supplemented with 10% fetal bovine serum (FBS, Gibco) and 1% penicillin-streptomycin (P/S, Gibco); MCF-7 cells were cultured in high-glucose DMEM (Gibco, 11965092) supplemented with 10% FBS and 1% P/S. All cells were incubated at 37°C in a humidified atmosphere containing 5% CO_2 (MDA-MB-231 and Hs 578T cells cultured in L-15 medium were maintained under CO_2-free conditions). When cells reached approximately 80–90% confluence, they were detached using 0.25% trypsin-ethylenediaminetetraacetic acid (trypsin-EDTA, Gibco) for subculture. All experiments were performed using cells in the logarithmic growth phase with passage numbers below 20.

Cell transfection

MDA-MB-231 cells were seeded into 96-well plates at a density of 5×10^3 cells per well [for methylthiazolyldiphenyl-tetrazolium bromide (MTT) and dual-luciferase reporter assays] or into 6-well plates at a density of 2×10^5 cells per well (for RNA and protein extraction, flow cytometry and Transwell assays) (Sun *et al*., 2025). After 24 hours of culture to allow cell adhesion, transfection was performed using Lipofectamine 3000 reagent (Invitrogen, L3000015) according to the manufacturer‘s instructions. Cells were at 60–70% confluence at the time of transfection. At 48 hours post-transfection, transfection efficiency was estimated by fluorescence microscopy following co-transfection with the pEGFP-N1 plasmid (Clontech) or by using a carboxyfluorescein (FAM)-labeled negative control miRNA (GenePharma). Transfection efficiency was >70% in all experiments. All experimental data were analyzed based on successfully transfected cells.For each well of a 96-well plate (100 μL total volume), the transfection

mixture contained 0.2 μL Lipofectamine 3000, 50 ng of miRNA mimic (miR-152-3p mimic or miR-NC, GenePharma) or a final concentration of 50 nM, diluted with Opti-MEM medium (Gibco) to a total volume of 10 μL. For 6-well plates, reagent volumes were scaled up proportionally. Culture medium was replaced with complete medium 6 hours post-transfection and cells were further cultured until the indicated time points for subsequent assays. At least three independent biological replicates were performed for each experimental group.TNBC cells were divided into the following groups: the mimic group (transfected with miR-152-3p mimics), the negative mimic group (transfected with miR-NC) and the blank group (MDA-MB-231 cells without any treatment). The miR-152-3p inhibitor group was transfected with miR-152-3p inhibitor and the inhibitor negative control group (Inhibitor-NC) was transfected with the inhibitor negative control sequence. Quantitative reverse transcription polymerase chain reaction (qRT-PCR) was performed to detect miR-152-3p transfection and expression levels. Laboratory members randomized cell seeding, transfection and treatment group assignments. Cell counting, image acquisition and data analysis were performed by another investigator who was blinded to the group allocations. The above experiments were conducted in parallel in MDA-MB-231, Hs 578T and MCF-7 cells.

qRT-PCR detection of miR-152-3p expression

Total RNA was extracted from MCF-10A and MDA-MB-231 cells using TRIzol reagent (Invitrogen) and reverse transcribed into complementary DNA (cDNA) using a Mir-X miRNA First-Strand Synthesis Kit (Takara). qRT-PCR was performed using SYBR Green Master Mix (Applied Biosystems) on a QuantStudio 5 system. Cycling conditions were as follows: 95°C for 5 min; 40 cycles of 95°C for 30 s, 54°C for 30 s and 72°C for 30 s. Relative miR-152-3p expression was calculated using the $2^{-}\Delta\Delta Ct$ method and normalized to glyceraldehyde-3-phosphate dehydrogenase (GAPDH) (Du *et al*., 2021). Primer sequences are listed in table 1.

MTT to detect cell proliferation ability

Cells were seeded and transfected in 96-well plates as described above. At the indicated time points (3, 6, 12, 24, and 48 h), 20 μL of MTT solution (5 mg/mL, Sigma, M2128) was added to each well, and the plates were incubated at 37°C for an additional 4 hours. The culture medium was carefully aspirated and 150 μL of dimethyl sulfoxide (DMSO, Sigma) was added to each well. Plates were shaken at low speed for 10 minutes to dissolve the formazan crystals fully. Absorbance was measured at 490 nm using a multi-mode microplate reader (BioTek Synergy H1). Blank wells containing no cells were used as background control. Relative cell viability was calculated using the formula: (ODtreatment − ODblank) / (ODcontrol − ODblank) × 100% (Wu *et al*., 2021). At least six technical replicates were set for each group at each time point and the experiment was independently repeated three times. These assays were performed in parallel in MDA-MB-231, Hs 578T and MCF-7 cells.

Flow cytometry to detect cell apoptosis

Flow cytometry was used to detect cell apoptosis (Sun *et al*., 2025). Cells were seeded in 6-well plates and harvested 48 hours post-transfection, including floating cells in the supernatant. Cells were digested with trypsin without EDTA and stained using the Annexin V-fluorescein isothiocyanate (FITC)/propidium iodide (PI) Apoptosis Detection Kit (BD Biosciences, 556547). Approximately 1×10^5 cells were resuspended in 100 μL of 1× binding buffer, followed by the sequential addition of 5 μL of Annexin V-FITC and 5 μL of PI solution and incubated at room temperature for 15 minutes in the dark. Immediately after incubation, 400 μL of 1× binding buffer was added and samples were analyzed within 1 hour using a flow cytometer (BD FACSCanto II). Data were processed using FlowJo software (v10.8.1). The total apoptosis rate was calculated as the sum of early apoptotic (Annexin V^+/PI^-) and late apoptotic (Annexin V^+/PI^+) cells. At least three independent biological replicates were performed for each group. These experiments were conducted in parallel in MDA-MB-231, Hs 578T, and MCF-7 cells.

Transwell assay to detect cell invasion ability

Transwell chambers (8.0 μm pore size, Corning, 3422) were pre-coated with Matrigel (Corning, 356234) diluted 1:8 in serum-free medium on ice. A total of 60 μL of diluted Matrigel was added to the upper chamber and incubated at 37°C for 4 hours to form a matrix gel. Cells transfected for 48 hours were resuspended in serum-free medium and seeded into the upper chamber at a density of 5×10^4 cells per well (total volume 200 μL). The lower chamber was filled with 600 μL of complete medium containing 20% FBS as a chemoattractant. Plates were incubated at 37°C under 5% CO_2 for 24 hours. The chambers were then removed and non-invaded cells on the upper surface were gently wiped off with a cotton swab. Invaded cells were fixed with 4% paraformaldehyde for 15 minutes and stained with 0.1% crystal violet for 20 minutes. Five non-overlapping fields (×200) were randomly selected and photographed under a microscope (Nikon Eclipse Ti2) and the number of invaded cells was counted (Zeng *et al*., 2021). Three independent chambers were used for each experimental condition and the entire experiment was independently repeated three times.

Dual luciferase reporter gene

To validate the direct targeting of candidate genes by miR-152-3p, dual-luciferase reporter assays were performed (Du *et al*., 2021). Putative conserved binding sites of miR-152-3p in the 3‘ untranslated regions (3’UTRs) of STAT3 (NM_139276.2), RELA (encoding NF-κB p65 subunit, NM_021975.3) and ADCY6 (adenylate cyclase 6, NM_015270.4) were predicted using TargetScan (release 7.2) and miRDB databases. Fragments of approximately

300–500 bp from the 3‘UTRs containing the predicted binding sites (wild-type, WT) were cloned into the XbaI site (downstream of the luciferase coding region) of the pGL3-Promoter vector (Promega, E1761), generating the following reporter plasmids: pGL3-STAT3-3’UTR-WT, pGL3-RELA-3‘UTR-WT and pGL3-ADCY6-3’UTR-WT. Subsequently, site-directed mutagenesis of the core seed region (complementary sequence of miR-152-3p) was performed using a QuikChange II XL Site-Directed Mutagenesis Kit (Agilent) to generate corresponding mutant (MUT) control plasmids: pGL3-STAT3-3‘UTR-MUT, pGL3-RELA-3’UTR-MUT and pGL3-ADCY6-3‘UTR-MUT. All constructed plasmids were verified by DNA sequencing. Taking STAT3 as an example, the predicted miR-152-3p binding site is located at nucleotides 1250–1256 of its 3’UTR (relative to NM_139276.2): wild-type sequence: 5‘-...ACUUUCA...-3’ (complementary to the miR-152-3p seed sequence 5‘-UGAAAGU-3’); mutant sequence: 5‘-...AGAAUCA...-3’.

Human embryonic kidney 293T (HEK-293T) cells were seeded into 96-well white plates at a density of 1×10^4 cells per well. After 24 hours of culture, co-transfection was performed using Lipofectamine 3000 transfection reagent. Each well contained 100 ng of the WT or MUT reporter plasmid described above, 20 ng of pRL-TK Renilla luciferase internal control plasmid (Promega, E2241) and 50 nM miR-152-3p mimic (sequence: UCAGUGCAUGACAGAACUUGG) or negative control miR-NC (sequence: UUCUCCGAACGUGUCACGUTT). Six replicate wells were set for each group. At 48 hours post-transfection, the medium was discarded, and luciferase activity was measured using the Dual-Luciferase® Reporter Assay System (Promega, E1910) according to the manufacturer’s instructions. Firefly luciferase activity (reporter) was measured first by adding Luciferase Assay Reagent II, followed by quenching and measurement of Renilla luciferase activity (internal control) upon addition of Stop & Glo® Reagent. Relative luciferase activity was calculated as the ratio of firefly luciferase activity to Renilla luciferase activity. Data from each group were normalized to the “wild-type reporter plasmid + miR-NC” group (set as 1.0). Six technical replicates (wells) were set for each transfection condition in a single experiment and the entire experiment was independently repeated three times.

Western blot to detect the protein expression levels of STAT3, RELA and ADCY6

Cells were lysed on ice for 30 minutes using radioimmunoprecipitation assay (RIPA) lysis buffer (Beyotime, P0013B) supplemented with protease and phosphatase inhibitors (Roche). Lysates were centrifuged at 12,000 g for 15 minutes at 4°C and supernatants were collected. Protein concentrations were determined using a bicinchoninic acid (BCA) protein assay kit (Thermo Scientific, 23227) and all samples were adjusted to equal concentrations with lysis buffer. Protein samples were mixed with 5× sodium dodecyl sulfate (SDS) loading buffer and denatured by boiling at 100°C for 10 minutes. A total of 30 μg of protein per lane was separated by 10% SDS-polyacrylamide gel electrophoresis (SDS-PAGE) under constant voltage (80 V for the stacking gel, 120 V for the separating gel). Proteins were transferred onto 0.45 μm polyvinylidene difluoride (PVDF) membranes (Millipore) using a wet transfer system at a constant current of 300 mA, with transfer time adjusted according to molecular weight (typically 90–120 minutes). Membranes were blocked with 5% non-fat milk (Bio-Rad) at room temperature for 1 hour and incubated with primary antibodies overnight at 4°C with gentle shaking (12–16 hours). The primary antibodies and dilutions used were as follows: STAT3 (rabbit monoclonal, 1:1000), NF-κB p65/RELA (rabbit monoclonal, 1:1000), ADCY6 (rabbit polyclonal, 1:500) and β-Actin (mouse monoclonal, internal control, 1:5000). The next day, membranes were washed three times with Tris-buffered saline containing Tween 20 (TBST) for 10 minutes each, then incubated with corresponding horseradish peroxidase (HRP)-conjugated secondary antibodies (goat anti-rabbit or anti-mouse, 1:5000) at room temperature for 1 hour. Membranes were washed again three times with TBST for 10 minutes each. SuperSignal™ West Pico PLUS chemiluminescent substrate (Thermo Scientific) was evenly applied to the membranes and images were captured using a chemiluminescence imaging system (Bio-Rad ChemiDoc MP). Densitometric quantification of bands was performed using Image Lab software (Bio-Rad). Relative expression levels of target proteins were calculated as: gray value of target protein band / gray value of corresponding internal control (β-Actin) band (Zeng *et al*., 2021). Each Western blot experiment included samples from all comparison groups and was performed with at least three independent biological replicates. The above experiments were conducted in parallel in MDA-MB-231, Hs 578T and MCF-7 cells.

STAT3 rescue experiment

To verify that miR-152-3p exerts its biological effects by targeting STAT3, a human STAT3 overexpression plasmid lacking the 3‘UTR (pcDNA3.1-STAT3) was constructed. MDA-MB-231 cells were seeded in 6-well or 96-well plates and co-transfected using Lipofectamine 3000 when cells reached 60% confluence. The experiment consisted of four groups: 1) miR-NC + empty vector; 2) miR-152-3p mimic + empty vector; 3) miR-NC + STAT3 overexpression; and 4) miR-152-3p mimic + STAT3 overexpression. The transfection amount of STAT3 plasmid was 500 ng/well and the transfection concentration of miRNA mimic was 50 nM. Cells were harvested 48 hours post-transfection for subsequent assays.

Statistical analysis

All data were processed using SPSS 27.0 software and results are expressed as mean ± standard error of the mean (SEM). All continuous data were first assessed for

normality using the Shapiro–Wilk test. For data that followed a normal distribution, one-way analysis of variance (ANOVA) was used for comparisons among more than two groups, followed by Tukey‘s post hoc test if the main effect was significant; comparisons between two groups were performed using an unpaired Student’s t-test. For data that did not follow a normal distribution, the Kruskal–Wallis test was used for comparisons among more than two groups, followed by Dunn‘s post hoc test if the main effect was significant; comparisons between two groups were performed using the Mann–Whitney U test. For multiple-group comparisons involving time-course factors, a two-way ANOVA was used to evaluate the main effects and interaction of the “treatment” and “time” factors. If the interaction was significant, Sidak’s multiple comparisons test was applied for between-group comparisons at each time point. The *n* in all experiments represents the number of independent biological replicates (e.g., independently cultured and treated cell batches). A p-value of less than 0.05 ($P < 0.05$) was considered statistically significant. Significance levels are indicated in the figures as follows: $*P < 0.05$, $**P < 0.01$, $***P < 0.001$.

RESULTS

qRT-PCR detection to compare miR-152-3p expression

The basal expression level of miR-152-3p was significantly lower in MDA-MB-231 cells compared to MCF-10A normal breast epithelial cells (**P* < 0.001, unpaired t-test, *n* =3), see Fig. 1.

Comparison of miR-152-3p expression of MDA-MB-231 cells

No significant difference in miR-152-3p expression was observed between the blank and miR-NC groups ($P > 0.05$).; miR-152-3p expression was significantly increased in the miR-152-3p mimic group compared with the blank group and the miR-NC group ($P<0.05$), see Fig. 2.

Cell proliferation ability comparison

Two-way ANOVA revealed that the main effects of both the treatment factor ($F = 68.3$, $**P < 0.001$) and the time factor ($F = 112.5$, $P < 0.001$), as well as their interaction ($F = 9.8$, $P < 0.001$), were statistically significant. Sidak's multiple comparisons test performed at each time point showed that, starting from 12 hours post-transfection, the proliferation rate in the miR-152-3p mimic group was significantly lower than that in the blank group ($*P = 0.011$), with more pronounced differences observed at 24 hours ($P < 0.001$) and 48 hours ($*P < 0.001$). No significant differences were observed between the blank group and the miR-NC group at any time point ($P > 0.05$) (n = 4 biological replicates, each with 6 technical replicates). See Fig. 3.

Comparison of apoptosis

There was no significant difference in apoptosis rate between the blank group and the miR-NC group ($P > 0.05$); however, the apoptosis rate was significantly higher in the miR-152-3p mimic group than in both control groups ($P < 0.05$; see Figs. 4 and 5).

Cell invasion ability comparison

The invasive ability of MDA-MB-231 cells in the blank group did not differ significantly from that in the miR-NC group ($P > 0.05$); however, the number of invaded cells was significantly lower in the miR-152-3p mimic group than in the blank and miR-NC groups ($P < 0.05$), see Figs. 6 and 7.

Effect of miR-152-3p loss-of-function on malignant phenotypes of TNBC cells

To further validate the functional necessity of endogenous miR-152-3p, loss-of-function experiments were performed using a miR-152-3p inhibitor. qRT-PCR analysis revealed that transfection with the miR-152-3p inhibitor significantly reduced endogenous miR-152-3p expression by approximately 65% compared to the Inhibitor-NC group ($P < 0.01$, Fig. 8A). Functional assays demonstrated that miR-152-3p knockdown induced phenotypic effects opposite to those observed upon miR-152-3p Overexpression: MTT assay showed that cell proliferative activity was significantly enhanced at 48 hours post-transfection in the miR-152-3p inhibitor group compared to the Inhibitor-NC group ($P < 0.01$, Fig. 8B); flow cytometry revealed a marked reduction in the apoptosis rate in the miR-152-3p inhibitor group ($P < 0.05$, Fig. 8C); and Transwell assay indicated that miR-152-3p knockdown significantly increased the invasive capacity of TNBC cells ($P < 0.01$, Fig. 8D).

Dual-luciferase reporter assay

Compared with the miR-NC control, co-transfection with miR-152-3p mimic significantly reduced the luciferase activity of wild-type (WT) 3'UTR reporter plasmids of STAT3, RELA and ADCY6 (all $P < 0.001$). However, this inhibitory effect of miR-152-3p mimic was completely abolished when the predicted miR-152-3p binding sites in the reporter plasmids were mutated (MUT) (all $P > 0.05$ vs. the corresponding MUT + miR-NC group). These results demonstrate that miR-152-3p suppresses gene expression by specifically binding to distinct sites within the 3’UTRs of STAT3, RELA (NF-κB p65) and ADCY6. See Fig. 9.

Western blot detection to compare STAT3, RELA and ADCY6 protein expression

One-way ANOVA revealed a statistically significant difference in STAT3 protein expression among the three groups ($F = 25.7$, $P = 0.001$). Tukey's post hoc test showed no significant difference between the blank group and the miR-NC group ($P = 0.962$), while STAT3 expression was significantly decreased in the miR-152-3p mimic group compared with both the blank group ($P = 0.001$) and the miR-NC group ($P = 0.001$) (n = 3). See Figs. 10 and 11.

Table 1: Primer sequence

mRNA	Gene	Primer sequence
miR-152-3p	F	5'-ACACTCCAGCTGGGTCAGTGCATGACAG-3'
	R	5'-CTCAACTGGTGTCGTGGAGTCGGCAATTCA-3'
GAPDH	F	5'-ATGGAGAAGGCTGGGGCTC-3'
	R	5'-AAGTTGTCATGGATGACCTTG-3'

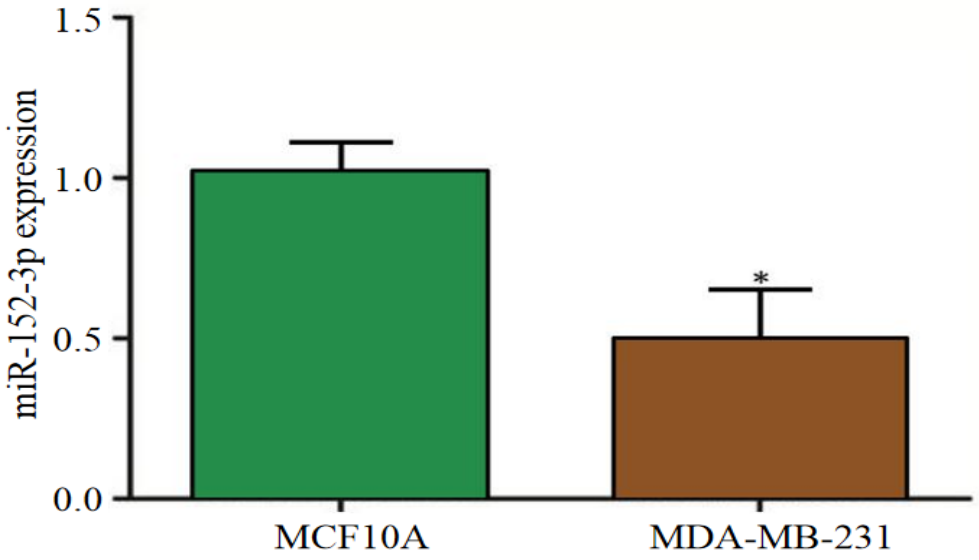

Fig. 1: Comparison of basal miR-152-3p expression levels between MCF-10A normal mammary epithelial cells and MDA-MB-231 triple-negative breast cancer cells
Note: Relative miR-152-3p expression was detected by qRT-PCR and normalized to GAPDH. *P < 0.05 indicates a significant difference compared with the MCF-10A group.

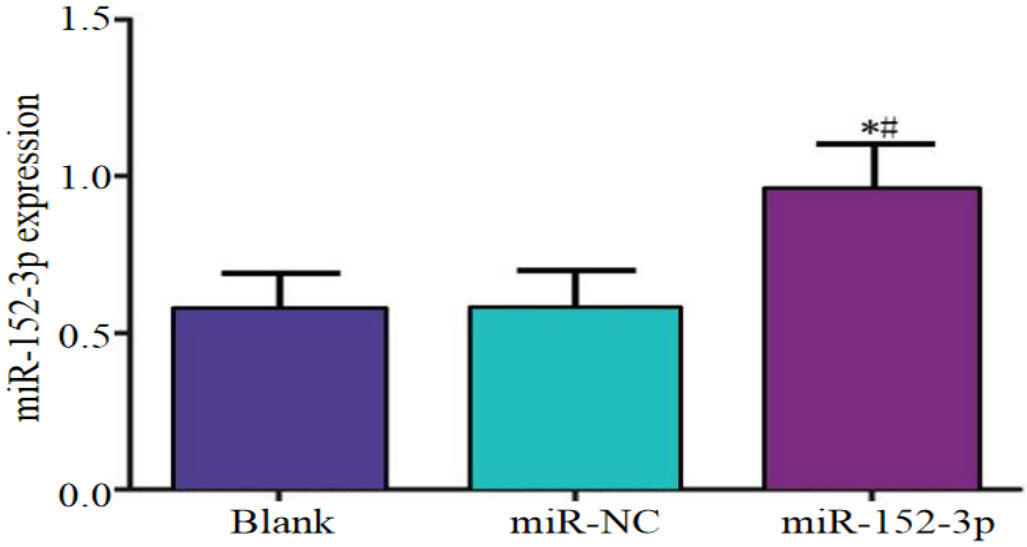

Fig. 2: Comparison of miR-152-3p expression levels in MDA-MB-231 cells after transfection with miR-152-3p mimic
Note: The experiment was divided into three groups: blank group (untreated), negative control group (transfected with miR-NC) and miR-152-3p mimic group (transfected with miR-152-3p mimic). *P < 0.05 indicates a significant difference compared with the blank group; #P < 0.05 indicates a significant difference compared with the miR-NC group.

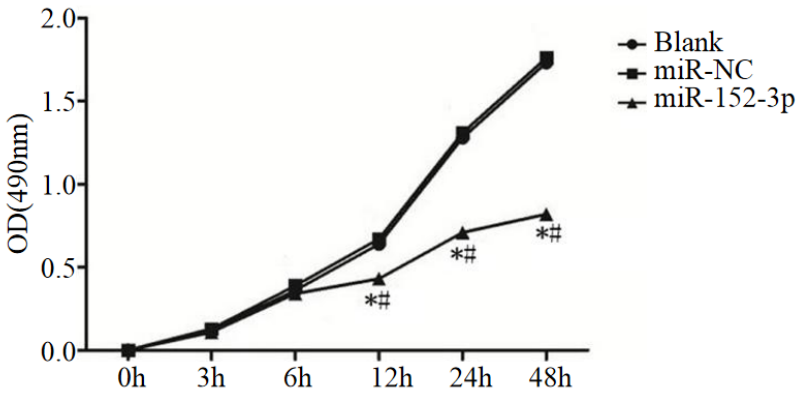

Fig. 3: Comparison of proliferative capacity of MDA-MB-231 cells among different treatment groups
Note: Cell proliferation was measured by MTT assay at various time points (3, 6, 12, 24 and 48 hours) post-transfection. Grouping is the same as in figure 2. *P < 0.05 indicates a significant difference compared with the blank group; #P < 0.05 indicates a significant difference compared with the miR-NC group.

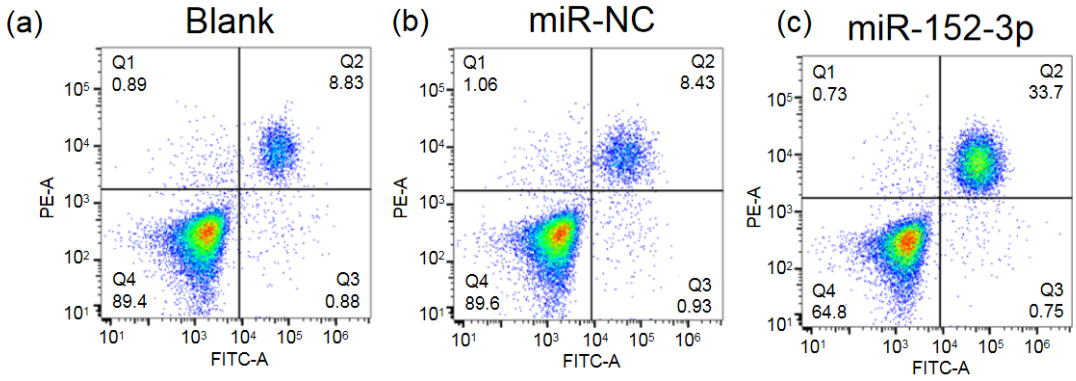

Fig. 4: Representative scatter plots of apoptosis in three groups of MDA-MB-231 cells detected by flow cytometry
Note: (a) Blank group (untreated); (b) Negative control group (transfected with miR-NC); (c) miR-152-3p mimic group (transfected with miR-152-3p mimic). Cells were stained with Annexin V-FITC and propidium iodide (PI). The lower left quadrant (Annexin V^-/PI^-) represents viable cells; the lower right quadrant (Annexin V^+/PI^-) represents early apoptotic cells; the upper right quadrant (Annexin V^+/PI^+) represents late apoptotic cells; the upper left quadrant (Annexin V^-/PI^+) represents necrotic cells. FITC, fluorescein isothiocyanate; PI, propidium iodide; miR-NC, negative control microRNA.

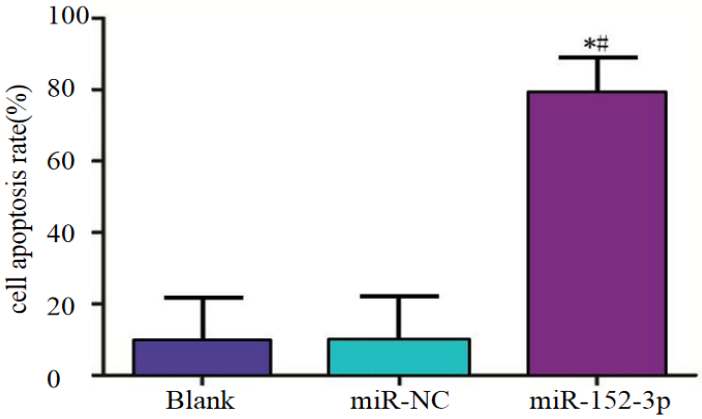

Fig. 5: Quantitative comparison of apoptosis rates in three groups of MDA-MB-231 cells
Note: Data represent mean ± SD from three independent experiments. *P < 0.05 indicates a significant difference compared with the blank group; #P < 0.05 indicates a significant difference compared with the miR-NC group.

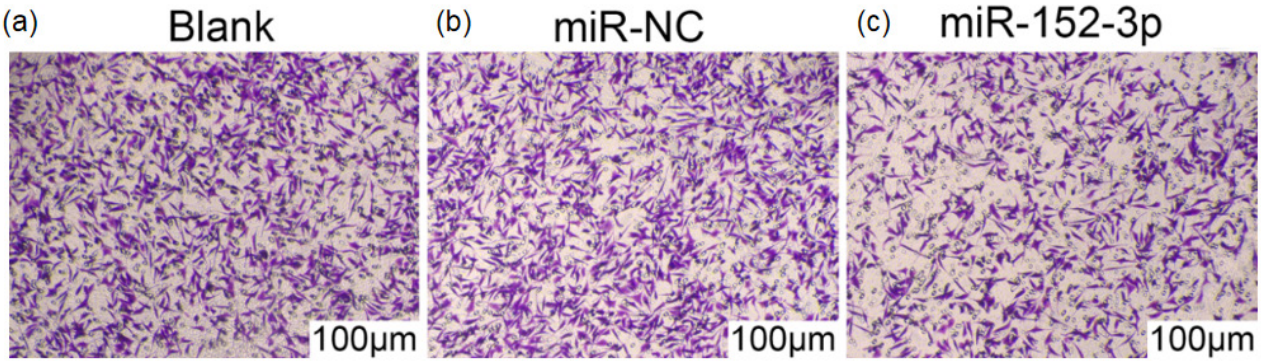

Fig. 6: Representative images of invasive capacity of three groups of MDA-MB-231 cells detected by Transwell assay (×200).
Note: (a) Blank group (untreated); (b) Negative control group (transfected with miR-NC); (c) miR-152-3p mimic group (transfected with miR-152-3p mimic). Cells that invaded through the Matrigel-coated membrane were stained with crystal violet. Scale bar = 50 μm. miR-NC, negative control microRNA.

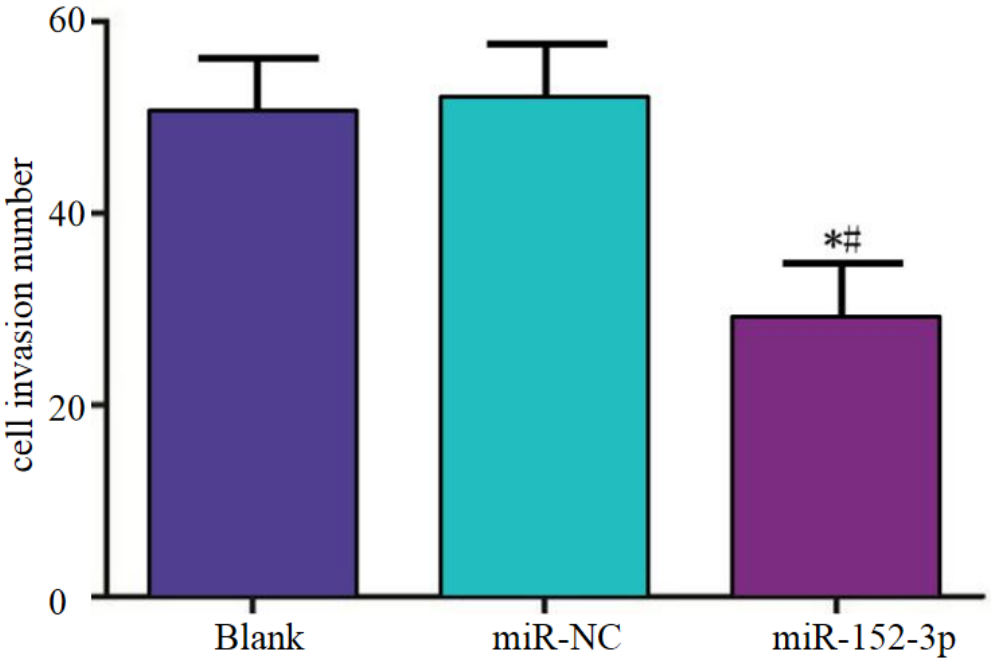

Fig. 7: Quantitative comparison of invaded cell numbers among three groups of MDA-MB-231 cells
Note: The number of invaded cells was counted per field, and the average was calculated from multiple fields. Grouping is the same as in Figure 2. *P < 0.05 indicates a significant difference compared with the blank group; #P < 0.05 indicates a significant difference compared with the miR-NC group.

STAT3 overexpression reverses the tumor-suppressive function of miR-152-3p

To provide direct evidence that miR-152-3p exerts its effects through STAT3, rescue experiments were performed. Western blot analysis showed that co-transfection of miR-152-3p mimic with a STAT3 overexpression plasmid lacking the 3'UTR successfully restored STAT3 protein expression levels (Fig. 12A). Functional assays demonstrated that STAT3 overexpression effectively reversed the phenotypic changes induced by miR-152-3p Overexpression: MTT assay revealed that cell proliferation capacity in the STAT3 overexpression group was significantly recovered compared with the miR-152-3p mimic alone group ($P < 0.01$, Fig. 12B); flow cytometry showed that STAT3 overexpression significantly attenuated the increased apoptosis rate induced by miR-152-3p mimic ($P < 0.05$, Fig. 12C). These results indicate that STAT3 is a key functional effector molecule downstream of miR-152-3p.

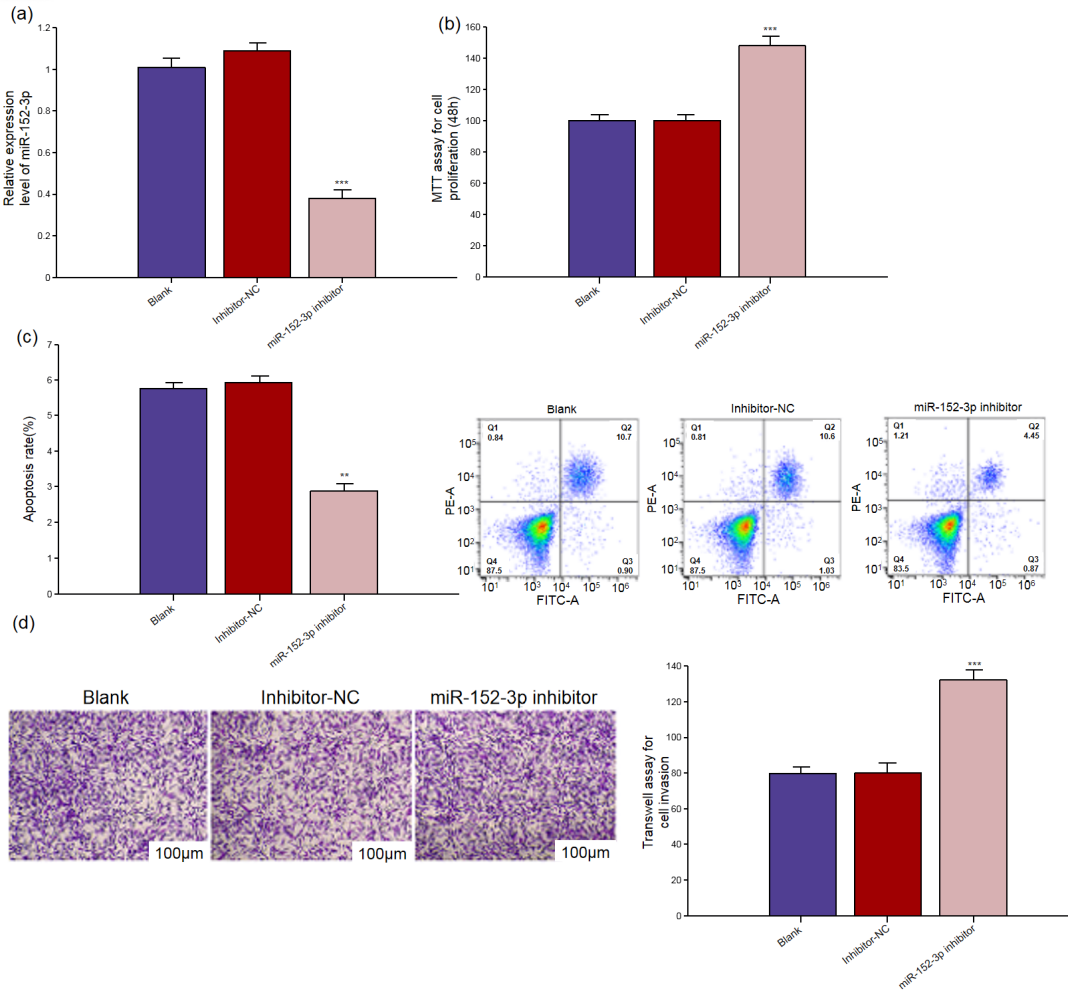

Fig. 8: Effect of miR-152-3p knockdown on malignant phenotypes of MDA-MB-231 cells
Note: (a) Relative miR-152-3p expression detected by qRT-PCR (n = 3); (b) Cell proliferation viability measured by MTT assay at 48 hours post-transfection (n = 5); (c) Apoptosis rate detected by flow cytometry, with representative scatter plots shown on the right (n = 3); (d) Quantification of invaded cells per field in Transwell assay (×100 magnification, n = 5). Data are presented as mean ± SD. *P < 0.05, **P < 0.01, ***P < 0.001 vs. Inhibitor-NC group. Inhibitor-NC, inhibitor negative control; qRT-PCR, quantitative reverse transcription polymerase chain reaction; MTT, methylthiazolyldiphenyl-tetrazolium bromide; SD, standard deviation.

Validation of miR-152-3p expression and function in multiple breast cancer cell lines

To further confirm the generality and subtype specificity of the miR-152-3p/STAT3 axis in breast cancer, parallel validation was performed using another TNBC cell line (Hs 578T) and an ER+ non-TNBC cell line (MCF-7). qRT-PCR analysis revealed that the basal expression level of miR-152-3p in Hs 578T cells was comparable to that in MDA-MB-231 cells, both of which were significantly lower than that in MCF-10A mammary epithelial cells ($P < 0.01$), whereas its expression level was relatively higher in MCF-7 cells (Fig. 13A). Overexpression of miR-152-3p in Hs 578T cells recapitulated the phenotypes observed in MDA-MB-231 cells: significant inhibition of cell proliferation ($P < 0.001$, Fig. 13B), induction of apoptosis ($P < 0.001$, Fig. 13C) and downregulation of STAT3 protein expression (Fig. 13D).

Dual-luciferase reporter assays confirmed that miR-152-3p also directly targeted the 3‘UTR of the STAT3 gene in Hs 578T cells (Fig. 13E). In MCF-7 cells, Overexpression of miR-152-3p induced only modest proliferation inhibition ($P < 0.05$, Fig. 13B) and apoptosis induction (Fig. 13C), with a weaker inhibitory effect on STAT3 protein expression (Fig. 13D).

DISCUSSION

TNBC is a highly-malignant breast cancer with poor prognosis and high mortality rate (Leon-Ferre and Goetz, 2023) and its treatment remains a clinical research focus. Non-coding miRNAs bind to target mRNAs, leading to translational repression or mRNA degradation, thereby inhibiting protein expression and, in turn, mediating cellular function and the growth and development of the organism (Billi *et al*., 2024).

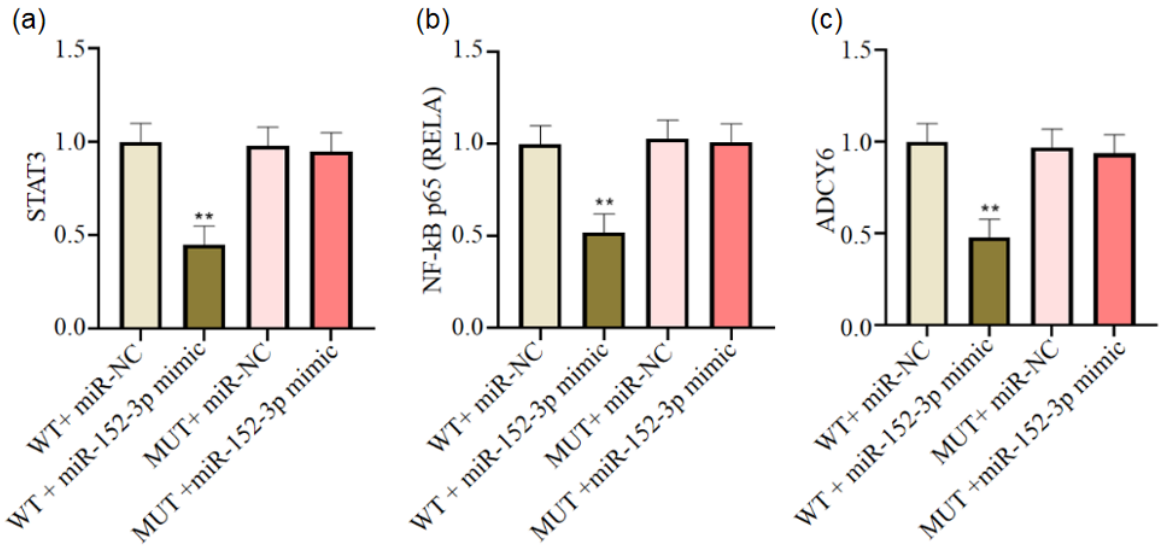

Fig 9: Validation of direct targeting of STAT3, RELA, and ADCY6 3'UTRs by miR-152-3p using dual-luciferase reporter assay

Note: (a) Relative luciferase activity of STAT3-3'UTR-WT and STAT3-3'UTR-MUT reporter plasmids; (b) Relative luciferase activity of RELA-3'UTR-WT and RELA-3'UTR-MUT reporter plasmids; (c) Relative luciferase activity of ADCY6-3'UTR-WT and ADCY6-3'UTR-MUT reporter plasmids. Experiments were performed in HEK-293T cells co-transfected with wild-type (WT) or mutant (MUT) 3'UTR reporter plasmids of the indicated genes, along with miR-152-3p mimic or negative control (miR-NC). Data were normalized to the relative luciferase activity of the "WT + miR-NC" group (set as 1.0) and are presented as mean ± SD (n = 6). *$P < 0.01$, **$P < 0.001$, ns, not significant (two-tailed Student's t-test). 3'UTR, 3' untranslated region; STAT3, signal transducer and activator of transcription 3; RELA, NF-κB p65 subunit; ADCY6, adenylate cyclase 6; HEK-293T, human embryonic kidney 293T cells; SD, standard deviation.

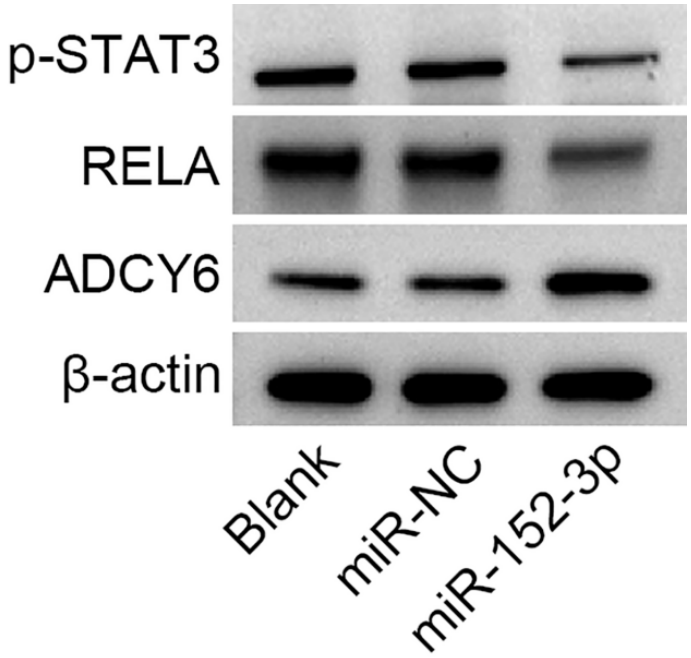

Fig. 10: Representative Western blot images of STAT3, RELA and ADCY6 protein expression in three groups of MDA-MB-231 cells

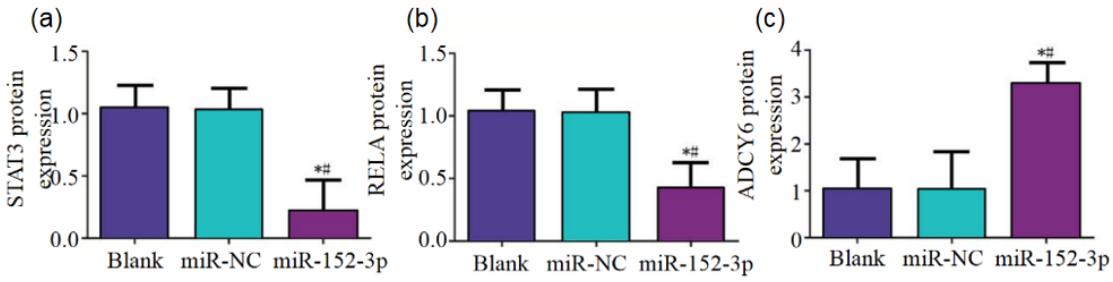

Fig. 11: Quantitative comparison of STAT3, RELA and ADCY6 protein expression in three groups of MDA-MB-231 cells

Note: (a) represents the comparison of STAT3 protein expression; (b) represents the comparison of RELA protein expression; (c) represents the comparison of ADCY6 protein expression. * Means P<0.05 compared with the blank group; # means P<0.05 compared with the miR-NC group. Data are presented as mean ± SD (n = 3 independent experiments, one-way ANOVA with Tukey's post hoc test).

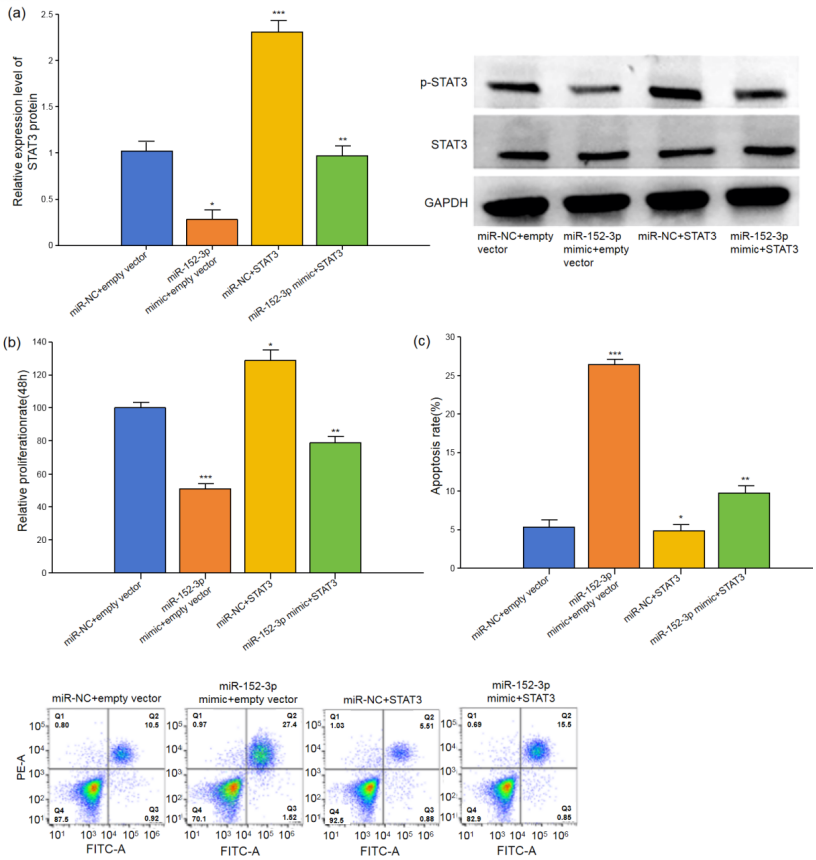

Fig. 12: Rescue experiment results of STAT3 overexpression reversing the inhibitory function of miR-152-3p

Note: (a) STAT3 protein expression detected by Western blot. β-Actin was used as a loading control; (b) Cell proliferation measured by MTT assay at 48 hours post-transfection; (c) Apoptosis induced by miR-152-3p and its reversal by STAT3 overexpression. Upper panel: Quantitative analysis of apoptosis rate detected by flow cytometry. Lower panel: Representative flow cytometry scatter plots. The experiment consisted of four groups: Group 1, miR-NC + empty vector; Group 2, miR-152-3p mimic + empty vector; Group 3, miR-NC + STAT3 overexpression plasmid; Group 4, miR-152-3p mimic + STAT3 overexpression plasmid. Cells were stained with Annexin V-FITC and propidium iodide (PI). The lower left quadrant (Annexin V^-/PI^-) represents viable cells; the lower right quadrant (Annexin V^+/PI^-) represents early apoptotic cells; the upper right quadrant (Annexin V^+/PI^+) represents late apoptotic cells; the upper left quadrant (Annexin V^-/PI^+) represents necrotic cells. Data are presented as mean ± SD. $P < 0.05$, *$P < 0.01$, **$P < 0.001$. STAT3, signal transducer and activator of transcription 3; miR-NC, negative control microRNA; MTT, methylthiazolyldiphenyl-tetrazolium bromide; FITC, fluorescein isothiocyanate; PI, propidium iodide; SD, standard deviation.

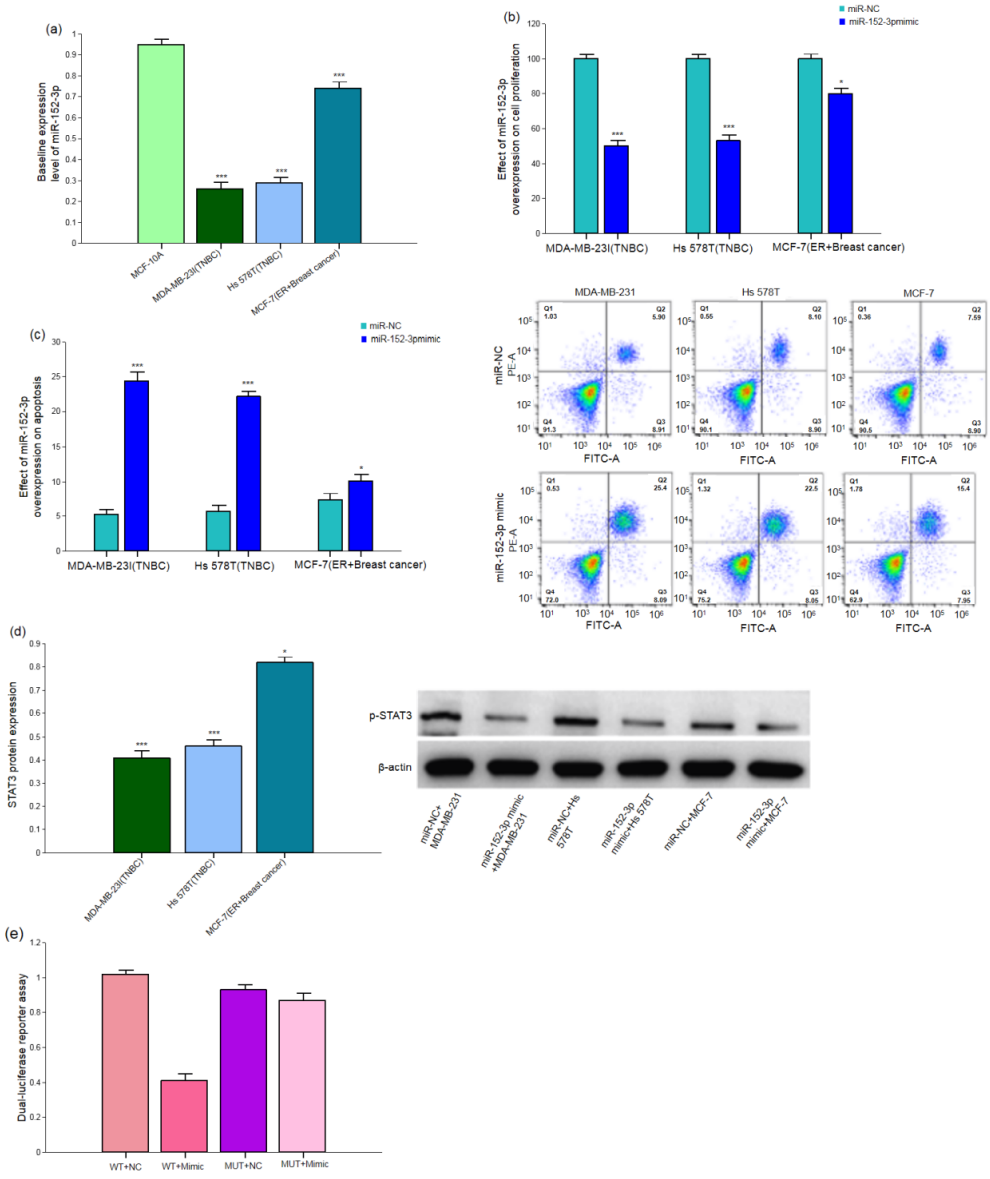

Fig. 13: Expression and functional validation of miR-152-3p in different breast cancer cell lines

Note: (a) Basal expression levels of miR-152-3p in MCF-10A normal mammary epithelial cells, MDA-MB-231 (TNBC), Hs 578T (TNBC), and MCF-7 (ER^+/PR^+, non-TNBC) cells detected by qRT-PCR. Data were normalized to GAPDH and are presented as mean ± SD (n = 3 independent experiments); (b) Effect of miR-152-3p overexpression on cell proliferation in MDA-MB-231, Hs 578T, and MCF-7 cells measured by MTT assay at 48 hours post-transfection. Cells were transfected with miR-152-3p mimic or negative control (miR-NC). Data are presented as mean ± SD (n = 5 independent experiments); (c) Effect of miR-152-3p overexpression on apoptosis in the indicated cell lines detected by flow cytometry. Left panel: Quantitative analysis of apoptosis rate. Right panel: Representative flow cytometry scatter plots (Annexin V-FITC/PI staining). Data are presented as mean ± SD (n = 3 independent experiments); (d) STAT3 protein expression changes in each cell line after miR-152-3p overexpression analyzed by Western blot. β-Actin was used as a loading control. Cells were transfected with miR-152-3p mimic or miR-NC for 48 hours. Representative blots from three independent experiments are shown; (e) Dual-luciferase reporter assay validating the direct regulatory effect of miR-152-3p on the STAT3 3'UTR in Hs 578T cells. Cells were co-transfected with wild-type (WT) or mutant (MUT) STAT3-3'UTR reporter plasmids, along with miR-152-3p mimic or miR-NC. Relative luciferase activity was normalized to the "WT + miR-NC" group (set as 1.0). Data are presented as mean ± SD (n = 4 technical replicates, experiment independently repeated three times). $P < 0.05$, *$P < 0.01$, **$P < 0.001$ (two-tailed Student's t-test for comparisons between miR-152-3p mimic and miR-NC groups within each cell line or each reporter construct). Abbreviations: TNBC, triple-negative breast cancer; ER^+, estrogen receptor-positive; PR^+, progesterone receptor-positive; qRT-PCR, quantitative reverse transcription polymerase chain reaction; GAPDH, glyceraldehyde-3-phosphate dehydrogenase; SD, standard deviation; MTT, methylthiazolyldiphenyl-tetrazolium bromide; miR-NC, negative control microRNA; FITC, fluorescein isothiocyanate; PI, propidium iodide; STAT3, signal transducer and activator of transcription 3; 3'UTR, 3' untranslated region; WT, wild-type; MUT, mutant.

Among the discovered miRNAs, its relationship with cancer is the focus of clinical research. Studies have shown that miRNAs not only regulate cancer cell activity but can also function as oncogenes or tumor suppressors. miR-152-3p is one of the most studied miRNAs in the miR-152 family and has attracted considerable attention as a tumor suppressor (Yin and Zhao, 2022). Studies have shown that miR-152-3p inhibits breast cancer cell proliferation and migration, potentially by regulating PIK3CA. However, the effect of miR-152-3p on the biological activity of TNBC cells remains poorly understood. Tumor cell migration ability reflects its metastatic potential. Cell invasion ability refers to the ability to penetrate blood vessels and can directly affect cell metastasis. The present study confirmed that miR-152-3p is downregulated in the classic TNBC cell lines MDA-MB-231 and Hs 578T, consistent with previous findings in breast cancer tissues (Dong *et al.,* 2025). In this study, miR-152-3p expression was significantly increased in the miR-152-3p mimic group, confirming successful transfection. The results demonstrated that the invasion and proliferation abilities of cells in the miR-152-3p group were weakened, while apoptotic ability was significantly enhanced. These findings indicate that miR-152-3p effectively regulates the biological activity of breast cancer cells and exerts tumor-suppressive effects. miR-152-3p plays a functionally essential tumor-suppressive role in TNBC and its mechanism of action may differ from traditional single-target paradigms, potentially involving the simultaneous modulation of multiple signaling nodes. Ning *et al*. (2024) found miR-152-3p inhibits melanoma metastasis by targeting NF-κB and confirmed that NF-κB is the main target of melanoma. Studies have shown that STAT3 is abundantly expressed in breast cancer cells and activated STAT3 is widely detected in human and animal breast cancer models (Zhou *et al*., 2024). The transcription factor NF-κB regulates the transcription of many genes. Elevated NF-κB expression has been reported in tumors and breast cancer cells (Zhang *et al*., 2022). Zuo *et al*. (2024) found that NF-κB expression was high in ER-negative breast cancer. cAMP is a critical second messenger that negatively regulates the cell cycle. The concentration of cAMP is often low in tumor tissues and peripheral blood, and it increases significantly after drug intervention (Campolo *et al*., 2022). This study found that STAT3 and RELA protein expression was reduced in miR-152-3p group cells. In contrast, ADCY6 protein expression was increased, indicating that miR-152-3p can effectively suppress the STAT3 and NF-κB (p65) pathways by targeting STAT3 and RELA, respectively, while potentially enhancing cAMP signaling by upregulating ADCY6 expression, thereby regulating the biological activity of breast cancer cells. Zhang *et al*. (2024) found, through animal experiments, that effective inhibition of genes regulated by the STAT3/NF-κB pathway can kill their receptors, thereby inhibiting proliferation, inducing chemosensitization, and hindering osteoclast formation. Kainat *et al*. (2026) confirmed that miR-152 inhibits breast cancer progression by targeting and regulating the DNMT1 gene.

The present study found that Overexpression of miR-152-3p significantly downregulated STAT3 and RELA (NF-κB p65) protein levels, accompanied by a marked increase in TNBC cell apoptosis. This observation is consistent with the established functions of STAT3 and NF-κB as key pro-survival transcription factors. Shao *et al*. (2023) reported that in chronic lymphocytic leukemia, IFN-γ secreted by T cells in the tumor microenvironment directly upregulates BCL-2 and MCL-1 expression via activation of the JAK1/2-STAT3 signaling pathway. Furthermore, activated NF-κB has been demonstrated to significantly upregulate various anti-apoptotic proteins, including IAPs, while suppressing the expression of pro-apoptotic genes, thereby enhancing cell survival (Calaf *et al*., 2024). Therefore, we hypothesized that miR-152-3p directly targets and inhibits STAT3 and RELA, thereby attenuating these two core survival signaling pathways. This may relieve their suppression of downstream apoptotic execution programs. It is worth emphasizing that the marked enhancement of apoptosis may result from the synergistic inhibition of both STAT3 and NF-κB by miR-152-3p. Future studies employing detection of Bcl-2 family protein expression changes, combined with pathway-specific inhibitors or agonists, will enable more precise dissection of the relative contributions and interaction networks of these pathways in miR-152-3p-mediated apoptosis.

Dual-luciferase reporter assays demonstrated that the miR-152-3p mimic specifically suppressed the reporter activity of constructs containing the wild-type 3'UTRs of STAT3, RELA, or ADCY6. In contrast, mutation of the predicted binding sites abrogated this inhibition. These findings provide preliminary supporting evidence for the hypothesis that miR-152-3p may regulate gene expression by directly binding the 3'UTRs of these genes. It should be emphasized that while this demonstrates the possibility of direct binding, complex post-transcriptional and translational regulatory mechanisms may exist between binding and the eventual changes in protein expression and functional phenotypes. Although this study confirmed, using dual-luciferase reporter assays, that miR-152-3p directly targets the 3'UTR of ADCY6 and observed upregulated ADCY6 protein expression, intracellular cAMP concentrations or downstream PKA pathway activity were not directly measured. Therefore, the mechanistic conclusions regarding miR-152-3p regulation of TNBC cell biological behavior through cAMP signaling remain primarily based on indirect evidence. Future studies should employ ELISA or FRET-based techniques to directly quantify cAMP levels, thereby providing more direct evidence of pathway activation. The STAT3 rescue experiments in this study showed that co-transfection with a STAT3 overexpression plasmid not subject to miRNA regulation partially reversed the miR-152-3p mimic-mediated inhibition of proliferation

and induction of apoptosis, suggesting that STAT3 is a key downstream effector mediating part of the tumor-suppressive functions of miR-152-3p. However, this study assessed only total protein levels of STAT3 and RELA, without detecting their phosphorylation status or nuclear translocation. Subsequent studies should use phosphorylation-specific antibodies for Western blot analysis to further confirm the inhibitory effect of miR-152-3p on STAT3/NF-κB pathway activity.

Furthermore, this core conclusion was successfully validated in another TNBC cell line, Hs 578T, confirming the universality of this regulatory axis across TNBC subtypes. Notably, in the ER+ non-TNBC cell line MCF-7, the tumor-suppressive effects of miR-152-3p Overexpression were significantly weaker than those observed in TNBC cells, suggesting that downregulation of miR-152-3p and the consequent dysregulation of the STAT3 pathway may represent characteristic molecular events contributing to the aggressive phenotype of TNBC. This provides an important theoretical basis for the future development of TNBC-specific miRNA-based therapeutics. This study identified STAT3, RELA, and ADCY6 as potential targets of miR-152-3p and suggests a possible synergistic mechanism in which a single microRNA can simultaneously modulate both oncogenic and tumor-suppressive signaling pathways, offering a promising therapeutic approach for TNBC, a malignancy characterized by high heterogeneity and a lack of single actionable targets.

CONCLUSION

In summary, the present study provides preliminary evidence at the cellular level that miR-152-3p exerts tumor-suppressive effects in TNBC by directly targeting and inhibiting STAT3 and RELA expression while simultaneously targeting and upregulating ADCY6 expression, thereby suppressing malignant phenotypes. These findings provide a foundation for subsequent investigations.

However, this study has limitations, including the absence of *in-vivo* validation, a narrow range of functional assays and an incomplete understanding of the synergistic mechanisms underlying multi-target regulation. The exact regulatory mechanisms and therapeutic potential of miR-152-3p require further validation through more comprehensive *in-vivo* and *in-vitro* studies.

Acknowledgments
None.

Authors' contributions
Yan Cheng: Research conception and design, experimental execution (cell culture, cell transfection, qRT-PCR, dual-luciferase reporter assay, Western blot, MTT assay, flow cytometry, Transwell invasion assay), data collection and organization, statistical analysis, figure preparation and drafting of the original manuscript; Yingyao Quan: Conceptualization and overall supervision of the study, guidance and optimization of experimental protocols, provision of key technical support and resources, data analysis and interpretation, manuscript review and revision and final approval of the version to be submitted.

Funding
There was no funding.

Data availability statement
The datasets generated and/or analyzed during the current study are available from the corresponding author upon reasonable request.

Ethical approval
This study was approved by the ethics committee of Anji County Traditional Chinese Medicine Hospital (Approval Number: 2025-105). This study was performed in adherence with the ARRIVE guidelines. See supplementary file for the ARRIVE checklist.

Conflict of interest
The authors declare that this research was conducted in the absence of any commercial or financial relationships that could be construed as potential conflicts of interest.

Supplementary data
https://www.pjps.pk/uploads/2026/05/SUP1778751300.pdf

REFERENCES

Arun S, Patel PK, Lakshmanan K, Rajangopal K, Swaminathan G and Byran G (2024). Targeting STAT3 enzyme for cancer treatment. *Mini Rev Med Chem*., **24**(13): 1252–1261.

Billi M, De Marinis E, Gentile M, Nervi C and Grignani F (2024). Nuclear miRNAs: Gene regulation activities. *Int J Mol Sci*., **25**(11): 6066.

Calaf GM, Crispin LA and Quisbert-Valenzuela EO (2024). Noscapine and apoptosis in breast and other cancers. *Int J Mol Sci*., **25**(6): 3536.

Campolo F, Capponi C, Tarsitano MG, Tenuta M, Pozza C, Gianfrilli D, Magliocca F, Venneri MA, Vicini E, Lenzi A, Isidori AM and Barbagallo F (2022). cAMP-specific phosphodiesterase 8A and 8B isoforms are differentially expressed in human testis and Leydig cell tumor. *Front Endocrinol (Lausanne)*., **13**: 1010924.

Deng L, Liao L, Zhang YL, Yang SY, Hu SY andriani L, Ling YX, Ma XY, Zhang FL, Shao ZM and Li DQ (2024). SF3A2 promotes progression and cisplatin resistance in triple-negative breast cancer via alternative splicing of MKRN1. *Sci Adv*., **10**(14): eadj4009.

Dong C, Sun Y, Xu X, Li H, Song X, Wei W, Jiao C, Xu H, Liu Y, Mierzhakenmu Z, Li L and Ma B (2025). c-Myc knockdown restores tamoxifen sensitivity in triple-negative breast cancer by reactivating the expression of ERα: the central role of miR-152 and miR-148a. *Breast Cancer*., **32**(3): 529–542.

Du C, Zhang J, Zhang L, Zhang Y, Wang Y and Li J (2021). Hsa_circRNA_102229 facilitates the progression of triple-negative breast cancer via regulating the miR-152-3p/PFTK1 pathway. *J Gene Med*., **23**(9): e3365.

Ethiraj P, Sasi B, Holder KN, Lin AP, Qiu Z, Jaafar C, Elkhalili A, Desai P, Saksena A, Ritter JP and Aguiar RCT (2022). Cyclic-AMP signalling, MYC and hypoxia-inducible factor 1α intersect to regulate angiogenesis in B-cell lymphoma. *Br J Haematol*., **198**(2): 349–359.

Gao Z, Lei WI and Lee LTO (2022). The role of neuropeptide-stimulated cAMP-EPACs signalling in cancer cells. *Molecules*., **27**(1): 311.

Giaquinto AN, Sung H, Newman LA, Freedman RA, Smith RA, Star J, Jemal A and Siegel RL (2024). Breast cancer statistics 2024. *CA Cancer J Clin*., **74**(6): 477–495.

Guo R, Liu T, Shasaltaneh MD, Wang X, Imani S and Wen Q (2022). Targeting adenylate cyclase family: New concept of targeted cancer therapy. *Front Oncol*., **12**: 829212.

Hu Y, Dong Z and Liu K (2024). Unraveling the complexity of STAT3 in cancer: Molecular understanding and drug discovery. *J Exp Clin Cancer Res*., **43**(1): 23.

Kainat N, Mansoor Q and Baig RM (2026). SNP-Driven LncRNA H19 dysregulation and CeRNA axis in breast and thyroid cancers among Pakistani females. *Mol Biol Rep*., **53**(1):409.

Leon-Ferre RA and Goetz MP (2023). Advances in systemic therapies for triple negative breast cancer. *BMJ*., **381**: e071674.

Mufidah N, Muzari K, Budi HS, Indrawati R, Anitasari S, Shen YK and Umarudin U (2025). Oral anticancer promising of hexadecanoic acid through melecular interaction to nuclear factor-kappa-B p65/RELA and tumor suppressor-p53. *Braz J Biol*., **85**: e287760.

Ning N, Tian Z, Feng H and Feng X (2024). Lnc NEAT1 facilitates the progression of melanoma by targeting the miR-152-3p/CDK6 axis: An observational study. *Medicine (Baltimore)*., **103**(44): e40379.

Patritti Cram J, Wu J, Coover RA, Rizvi TA, Chaney KE, Ravindran R, Cancelas JA, Spinner RJ and Ratner N (2022). P2RY14 cAMP signaling regulates Schwann cell precursor self-renewal, proliferation and nerve tumor initiation in a mouse model of neurofibromatosis. *Elife*., **11**: e73511.

Sammons SL, Sanglier T, Leone JP, Erick TK, Lambert P, Montemurro F, Poppe R, Restuccia E, Tolaney SM and Lin NU (2025). Prevalence by therapy line and incidence of breast cancer brain metastases in 18 075 patients. *J Natl Cancer Inst*., **117**(8): 1565–1572.

Shao X, Meng X, Yang H, Wang X, Qin L, Shen G, Xi X, Zhao H, Macip S and Chen Y (2023). IFN-γ enhances CLL cell resistance to ABT-199 by regulating MCL-1 and BCL-2 expression via the JAK-STAT3 signaling pathway. *Leuk Lymphoma*., **64**(1): 71–78.

Sun Y, An L, Kong L, Liu X, Zhang H, Liu J and Qian P (2025). MiR-518c-5p/miR-4524a-3p can mediate immune escape and chemotherapy resistance in triple-negative breast cancer and predict its outcome. *Hereditas*., **162**(1): 216.

Turijan-Espinoza E, Ruiz-Rodriguez VM, Paz-Rodriguez VA, Hernandez-Hernandez GE, Hernandez-Gonzalez O, Guel-Panola JA, Zermeno-Nava JJ, Gutierrez-Gil MC and Portales-Perez DP (2026). Profiles of microRNAs in patients with advanced breast cancer who are chemoresistant or chemosensitive to fluorouracil, adriamycin and cyclophosphamide treatment. *Asian Pac J Cancer Prev*., **27**(2):469–479.

Wu J, Xu W, Ma L, Sheng J, Ye M, Chen H, Zhang Y, Wang B, Liao M, Meng T, Zhou Y and Chen H (2021). Formononetin relieves the facilitating effect of lncRNA AFAP1-AS1-miR-195/miR-545 axis on progression and chemo-resistance of triple-negative breast cancer. *Aging (Albany NY)*., **13**(14): 18191-18222.

Yang B, Huang S, Chen H, Li R, Hou S, Zhao J and Li Y (2022). DNMT3B regulates proliferation of A549 cells through the microRNA-152-3p/NCAM1 pathway. *Oncol Lett*., **23**(1): 11.

Yin T and Zhao H (2022). miR-152-3p impedes the malignant phenotypes of hepatocellular carcinoma by repressing roundabout guidance receptor 1. *Cell Mol Biol Lett*., **27**(1): 22.

Zeng X, Ma X, Guo H, Wei L, Zhang Y, Sun C, Han N, Sun S and Zhang N (2021). MicroRNA-582-5p promotes triple-negative breast cancer invasion and metastasis by antagonizing CMTM8. *Bioengineered*., **12**(2): 10126-10135.

Zhang M, Liu ZZ, Aoshima K, Cai WL, Sun H, Xu T, Zhang Y, An Y, Chen JF, Chan LH, Aoshima A, Lang SM, Tang Z, Che X, Li Y, Rutter SJ, Bossuyt V, Chen X, Morrow JS, Pusztai L and Yan Q (2022). CECR2 drives breast cancer metastasis by promoting NF-κB signaling and macrophage-mediated immune suppression. *Sci Transl Med*., **14**(630): eabf5473.

Zhang Z, Li B, Wu S, Yang Y, Wu B, Lai Q, Lai F, Mo F, Zhong Y, Wang S, Guo R and Zhang B (2024). Bergenin protects against osteoarthritis by inhibiting STAT3, NF-κB and Jun pathways and suppressing osteoclastogenesis. *Sci Rep*., **14**(1): 20292.

Zhou X, Zhao J, Yan T, Ye D, Wang Y, Zhou B, Liu D, Wang X, Zheng W, Zheng B, Qian F, Li Y, Li D and Fang L (2024). ANXA9 facilitates S100A4 and promotes breast cancer progression through modulating STAT3 pathway. *Cell Death Dis*., **15**(4): 260.

Zuo X, Zhao X, Zhang X, Li Q, Jiang X, Huang S, Chen X, Chen X, Jia W, Zou H, Shi D and Qian X (2024). PTPN20 promotes metastasis through activating NF-κB signaling in triple-negative breast cancer. *Breast Cancer Res*., **26**(1): 155.